Journal of Materials and Environmental Science
ISSN : 2028-2508
e-ISSN : 2737-890X
CODEN : JMESCN

J. Mater. Environ. Sci., 2022, Volume 13, Issue 05, Page 576-598

http://www.jmaterenvironsci.com

Experimental and Theoretical Evaluation Of Corrosion Inhibition of Honeycomb Propolis Extract On Mild Steel In Acidic Media

Ibrahim Abdullahi Idris [1], Abdullahi Umar Bello[2], Bishir Usman*[1],

[1]*Department of Pure and Industrial Chemistry, Faculty of Physical Sciences, College of Natural and Pharmaceutical Sciences, Bayero University, Kano Nigeria, P.M.B 3011.*

[2]*Department of Chemistry, Faculty of Science, Ahmadu Bello University, Zaria, Kaduna State*

**Corresponding author, Email address: busman.chm@buk.edu.ng*

Received 13 May 2022,
Revised 28 May 2022,
Accepted 30 May 2022

Keywords
- *Corrosion Inhibition*
- *Honey comb propolis,*
- *Experimental,*
- *Quantum Chemical Calculations ,*
- *Molecular dynamic Simulations.*

Busman.chm@buk.edu.ng
Phone: +2348065642704;

Abstract

The inhibition performance and adsorption effect of ethanolic extract of Honeycomb propolis (HP) on the corrosion of mild steel in 0.5M H_2SO_4 has been investigated using weight loss measurement and quantum chemical calculation. The results obtained show that the inhibition efficiency from the weight loss studies was found to be 95.11% at optimum concentration of 5000ppm of Honeycomb propolis extract and Inhibition efficiency was found to increase with increasing concentration of the extract and also decrease with rise in temperature. values of activation energies such as Ea, ΔH, ΔG and ΔS, shows the negative values of ΔS as a decrease in disorder that took place when going from reactant to activated complex, the negative values of ΔG suggests spontaneous and feasible adsorption process. Furthermore, Adsorption behavior of the extract on the mild steel surface was found to be physisorption and closely Freundlich adsorption isotherm. Adsorbed film of inhibitor at metal solution interface has been confirmed using FTIR. GC-MS analysis was performed to find the active component responsible for the corrosion inhibition,and the ethanolic extract of honeycomb propolis is reach in several constituent such as 9,12-octadecadienal (27.59%), 9-octadecenoic acid, ethyl ester (19.02%), Hexadecanoic acid, ethyl ester (10.64%) and Linoleic acid ethyl ester (9.92%).Scanning electron (SEM) studies also provide the confirmatory evidence of an improved surface condition in the presence of the HP Extract owing to the adsorption process. UV-visible spectroscopy analysis confirmed the formation of Fe-Inhibitor complexes. The of quantum chemical calculations and Molecular Dynamic (MD) simulation was used and the results confirmed the good inhibition performance of HP extract due to its high E_{HOMO} value, lower E_{LUMO} value, and low energy gap indicating its ease ability in offering and accepting electrons. Molecular dynamic simulation shows negative values of binding energy that is less than 100Kcalmol^{-} which suggests physical adsorption.

1. Introduction

Corrosion of metals is a worldwide scientific problem as it has an effect on highways, [1] bridges, buildings, oil and gas, chemical processing, water and waste water treatment and almost on all metallic objects in use which therefore, set in place a serious threat to the environment and human health [2,3,4]. Corrosion is also an electrochemical phenomenon which includes the transfer of electrons between a metal surface and an aqueous solution. There are many methods and strategies for metal protection against corrosion. However, corrosion cannot be fully prevented completely since it is constant and continuous problem, therefore, corrosion control becomes an option which involves the slowing of its kinetics and/or altering its mechanism [5]. Mild steels are widely the metal used in many industries application due to their excellent mechanical properties and low cost. However, when exposed to aggressive environments, such as the use of acid solutions for pickling, industrial acid cleaning, cleaning of oil refinery equipment, oil well acidizing and acid descaling, these processes usually lead to substantial loss of the metal due to corrosion [2,6,7]

Various methods have been used to prevent destruction or degradation of metal surface, the corrosion inhibitor application is one of the best-known methods of corrosion protection and one of the most accepted in the industries [8,9]. The majority of highly effective inhibitors used in oil and gas industry are organic compounds containing one or more hetero atoms; such as oxygen, nitrogen, and sulfur atoms conjugated with multiple bonds within the molecular structure [10-11]. This method is considered best due to low cost and practical applications involved [12-14]. In view of this development, the bee products Honeycomb Propolis Extract are other natural materials that might be efficiently used for the protection of metals and alloys against corrosion. Honeycomb Propolis Extract will be investigated in this research work as corrosion inhibitor. Propolis is one of the Honeycomb (bee) products which has gained the attention of scientist across the world recently due to its vast health benefits. The composition of propolis depends on the place and time of collection and varies greatly with the vegetal source that bees are using as raw material [15]. More than 160 components have been identified so far, among which phenolic compounds, including flavonoids, are the major components [16]. Propolis is currently widely used in medicine due to its antibacterial, antiviral, antifungal and antioxidant properties. Research shows that the inhibition potentials of any inhibitor are also influenced by electronic and molecular properties of the inhibitor. As such, the principle of quantum chemical studies shall be used to correlate microscopic and macroscopic properties of the inhibitors.

2. Materials and methods

2.1 Sample collection and preparation

The container used for the Honeycomb sampling was polythene bags. Honeycomb were collected from Utai district of wudil local government area, Kano State, Nigeria. The honey comb is pure containing zero amount of honey. The samples were washed with tap water then with double-distilled water and shade dried for 14 days and eventually ground to fine powder and stored. 750 g of the ground powder Honey comb was mixed with 3 litre of ethanol in a clean dark coloured plastic container. And the container was sealed fellow by shaking once or twice a day. The plastic container was kept in a worm dark place to achieved best results, for the period of two weeks. After two weeks, the liquid was filtered through a clean and very fine cloth fellow by second filtration with Whiteman filter paper. The filtrates was kept in a freezer at –10 °C overnight and then filtered again to reduce the wax content of the extracts. The solution was evaporated using a Rotary evaporator, Model R-210, at a temperature of 48^{o}C to obtain the concentrated crude extract. The extract obtained after the evaporation of ethanol was assumed to be 100% concentrated. The solvent was evaporated in a vacuum oven at a temperature of 60 °C to obtain dry paste like form ethanolic extract. The crude extract was stored in a clean bottle and covered properly [17]. The mild steel was cut mechanically into many coupons, each of dimension 2cm x 2cm x 0.2cm for weight loss studies. Prior to analysis, the test coupons were prepared for corrosion experiments by abrading them with different grades (600-1200) of Emery paper, then washed in ethanol, degreased in acetone, and dried in air. The coupons were then weighed and stored in a desiccator prior to corrosion analysis.

2.2 **Weight loss measurement**

The Weight loss experiment was conducted in accordance with ASTMG 1-03 standard procedure in the weight loss study. The Honeycomb extract 0.05g, 0.1g, 0.15g, 0.2g and 0.25g were dissolved ina conical flask containing 50ml 0.5M H_2SO_4 acid solutions to obtain concentration of 1000, 2000, 3000, 4000 and 5000ppm. The test samples were immersed in the flask for about (1,2,3 and 4hrs) at different temperatures 303-333K. After immersion time, the coupons were brought out of the solution, cleaned with distilled water and dried in an oven for 10mins. To obtain the Weight loss, the mass obtained after the experiment was subtracted from the mass before the experiment, it was also possible to determine the inhibition efficiency IE%, surface coverage (θ) and corrosion rate C_R using equations 1,2 and 3 respectively [18].

$$\%I = \left(1 - \frac{w1}{w2}\right) \text{ x } 100 \qquad (1)$$

where W^1 and W^2 are the corrosion rate of mild steel specimens obtained in sulfuric acid, with and without plant extracts, respectively.

The degree of coverage of the surface (θ) of mild steel by molecules of the inhibitor can be expressed as using equation (2) [18].

$$\theta = 1 - \frac{w1}{w2} \qquad (2)$$

The expression for measurement of corrosion rate (C.R) in millimeters penetration per year (mm/y) was used to measure corrosion rate (C.R) for the specimens, which was expressed in equation (3) [58]

$$C_R = \frac{86.4 \ x\, W}{\alpha t \rho} \qquad (3)$$

Where, w is corrosion weight loss of mild steel (mg), α is the total surface area of the specimen in (cm^2), t is the exposure time in hours (hr), ρ is the density of the specimen (g/cm^3).

2.3 Scanning electron microscopy

The surface condition of the coupons in contact with 0.5M H_2SO_4 acid solutions in the absence and presence of the inhibitors were analyzed with the aid of Phenom World, Scanning Electron Microscope of Model PW-100-012 with serial no: MVE015707775 and model number: 800-07334 SEM is a type of electron microscope that produces images of a sample by scanning it with a focused beam of electrons. The electrons interact with atoms in the sample, producing various signals that can be detected and that contain information about the samples surface topography and composition. The electron beam is scanned in a raster scan pattern, and the beam position is combined with the detected signal to produce an image.

2.4. FTIR

Spectrometer model Carry 630 FTIR of the Agilent Technologies was used to carry out the structural characterization of the pure Honeycomb propolis extract and the corrosion products after the adsorption on the mild steel surface. The functional groups were investigated in the region of 4000-500 cm^{-1} (wave number), and identified by comparison with standard peaks position of the groups in literature.

2.5. UV

The optical characterization for the extract was performed by Perkin Elmer, lambda 35, UV-visible Spectrometer. In the process, a 0.2 mg of *Honeycomb propolis* extract leaves extract was mixed in 2.5 cm^3 of double distilled water, and the prepared solution was examined (Scanned) in the wavelength range 200-600 nm. The stability of the inhibitor molecules on the mild steel surface was investigated by immersing the specimen separately in the solution containing 0.5M H_2SO_4 (100 cm^3) with effective concentration of *Honeycomb propolis* extract. After 4h the test sample was removed from the solution, cleaned with distilled water, dip-washed thrice, and then immersed for half an hour in distilled water followed by smooth rubbing of the mild steel surface. This solution was examined again, and the results were compared with spectrum of the pure extract [19].

2.6 UV

Agilent Mass Hunter 19091S-433UI HP-5ms Ultra Inert GC system was used for GC-MS evaluation of Natural product contents of the Honeycomb propolis extract. The carrier gas was helium about 10 µL of the honeycomb extract in a mixture with ethanol were analysed using ultra inert GC. The temperature was placed at 500°C and kept for 2 minutes, the temperature was further increased to 180°C (with a rate of 20°C/min) and maintained for 5 minutes. Eventually, the temperature was escalated to 325°C (with a rate of 20°C/min) and stabilised for 5 minutes. The compounds were selected based on the comparison from the National Institute of Standards and Technology (NIST14) library the compounds that showed high percentage similarity with chemical compounds from NIST were selected for this study.

3. Results and Discussion

3.1 Effect of immersion time

Figure 1 shows the effect of immersion time on the weight loss of mild steel in solutions of 0.5M H_2SO_4in the absence and presence of various concentrations of Honeycomb propolis extract at 303K. It is evident that weight loss of mild steel decreases with increase in the concentration of the HPE but increases with increasing period of contact. This result clearly shows that as the concentration of the extract increases, the weight loss of the mild steel decreased, forming a protective layer on the surface [20,21].

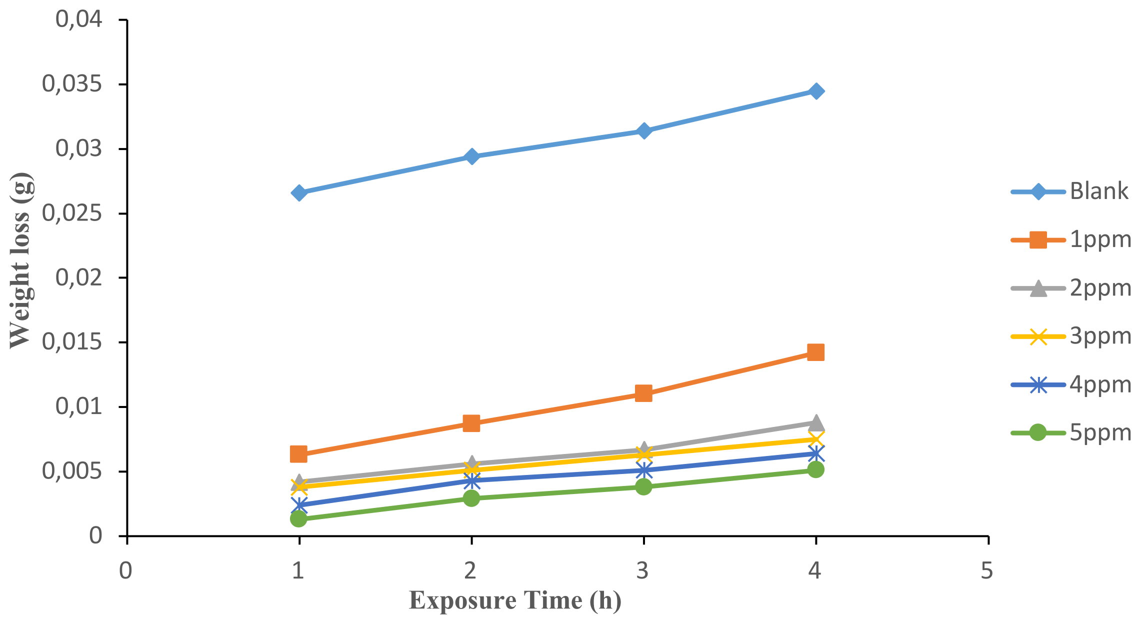

Figure 1: Variation of weight loss with time for the corrosion of mild steel in 0.5M H_2SO_4 containing various concentrations of *Honeycomb propolis* extract at 303K.

Figure 2 presents the inhibition efficiencies of mild steel at303K, 313K, 323K and 333K respectively, the results obtained revealed that the inhibition efficiency increases with increasing honeycomb propolis extract concentration up to 95.11% at 303K. At 303, 313, 323 and 333K maximum inhibition efficiencies 95.11%, 87.37%, 83.62% and 72.60% were obtained in 0.5M H2SO4 solution containing 5000ppm honeycomb propolis extract, respectively). These results were in agreement with that of [20-

22]. The results also indicate that the extract is an adsorption inhibitor that formed a protective layer on the surface of the mild steel. This finding conforms to that of [20-21].

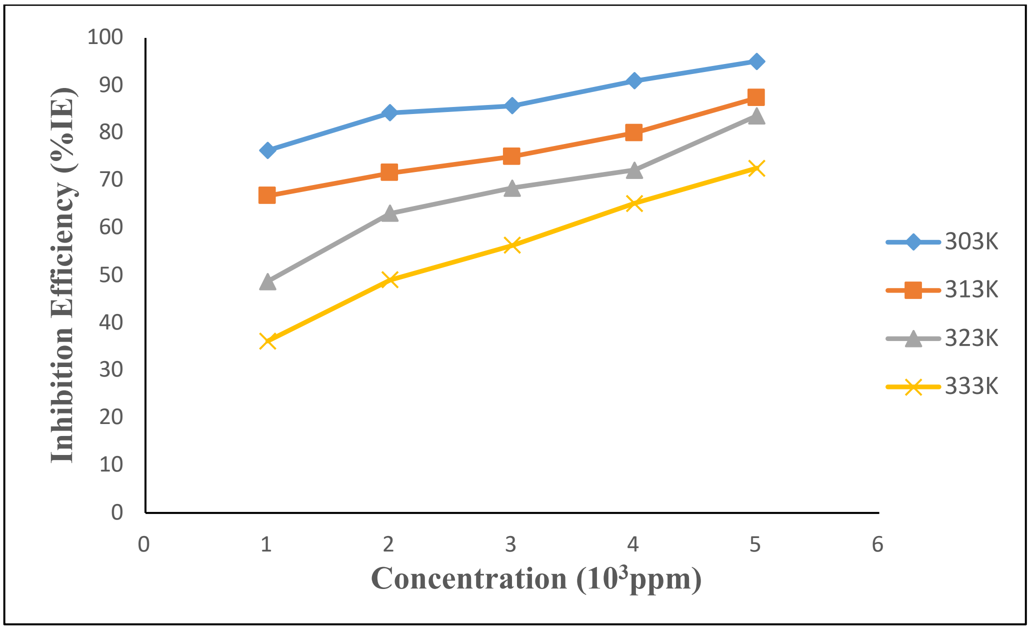

Figure 2: Variation of Percentage inhibition efficiency (%IE) at various concentration of *Honeycomb propolis* extract at different temperature.

3.2 Effect of temperature

Relationship between temperature and inhibition efficiency has been found to be an inverse relationship from Figure 3. That is, as the temperature goes up, the inhibition efficiency goes down. 95.11% was observed to be the highest at 303K with 72.60% as the lowest at temperature of 333K. This was also evident from figure 3. The increase and decrease may be attributed to a possible distortion of the adsorption–desorption equilibrium toward desorption of the already adsorbed inhibitor [23]. It may be also considered as change in kinetic energy of the reacting molecules because at higher temperature the inhibitor molecules were not very stable. These findings are in agreement with that of [24,25].

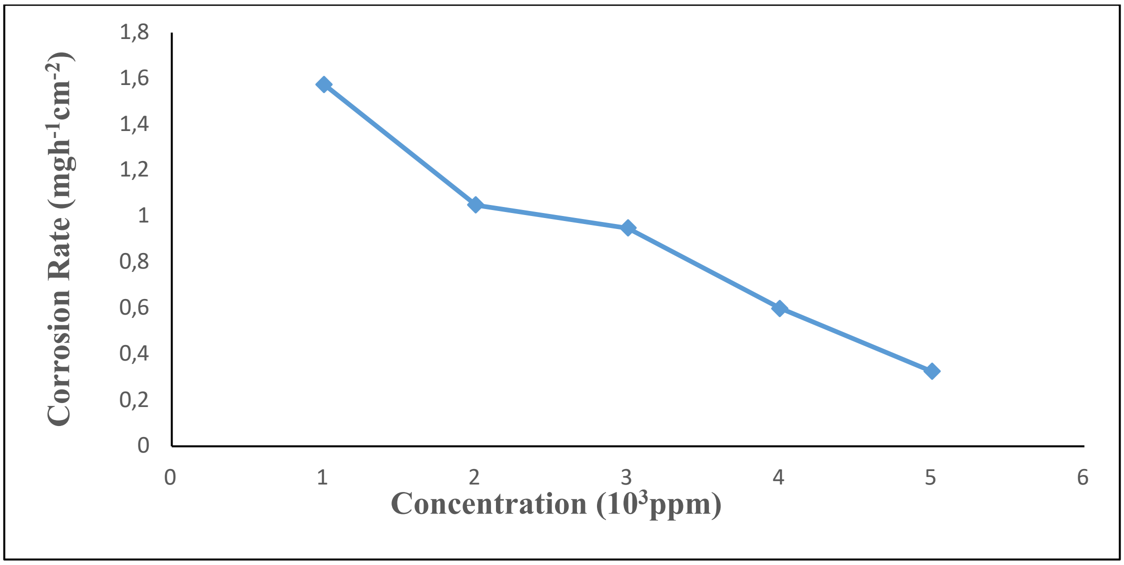

Figure 3: Corrosion Rate of mild steel against Various Concentrations of *Honeycomb propolis* extract in 0.5M H_2SO_4 at 303K.

3.3 Thermodynamic and Adsorption study

This is the minimum energy reacting molecules must possess before a chemical reaction can take place [26]. The corrosion rate of mild steel in Sulfuric acid and the temperature were related by the Arrhenius equation in equation (5). If the corrosion rates of the metal at temperatures, 303, 313, 323 and 333K are known, (i.e C_{R1}, C_{R2}, C_{R3} *and* C_{R4} respectively), then equation (6) can be Linearize to gives equation (9) [27]

$$C_R = A exp^{-Ea/RT} \quad 5$$

$$1nC_R = 1nA - \frac{E_a}{RT} \quad 6$$

Where C_R = corrosion rate, A= Arrhenius constant, R= Molar gas constant (8.314 J/molK), and T = Kelvin temperature.

Table 1 represents the results obtained from the kinetics parameters for the dissolution of mild steel in 0.5M H_2SO_4 in the absence and the presence of Honeycomb propolis extract at 303 K from which the values foe the apparent activation energies for the corrosion process in the presence of the extract were higher than that in the absence of the extract (blank). The increase in activation energies shows physical adsorption is taking place with the formation of an adsorptive film on the surface of the mild steel that protects it from the acidic medium. This conforms to the findings of [22-28]. Also, the optimum activation energy obtained was 79.64 $kJmol^{-1}$ which is an indication that the activation energy is lower than the threshold value of 80 $kJmol^{-1}$ [29] required for the mechanism of chemical adsorption, confirming a physical or columbic type of adsorption which is characterized by decrease in inhibition efficiency with a rise in temperature [30-31,35].

Table 1. Thermodynamic and kinetic parameters calculated from weight loss measurement.

Concentration (10^3ppm)	E_a ($kJmol^{-1}$)	ΔH_a ($kJmol^{-1}$)	ΔS_a ($Jmol^{-1}$)
Blank	53.44	50.79	-71.80
1	69.71	67.07	-25.43
2	75.93	73.29	-8.07
3	77.43	74.79	-6.69
4	77.68	75.03	-4.24
5	79.64	77.00	-2.27

Enthalpy is the sum of the internal energy of the system plus the product of the pressure of the gas in the system and its volume while entropy is the measure of disorderliness of a system [27] The thermodynamic parameters for the enthalpy of adsorption and entropy of the inhibitors on the mild steel (ΔH_a) and (ΔS_a) in the presence and absence of inhibitors was calculated using the transition state equation (5) [27]:

$$= 1n\left(\frac{R}{Nh}\right) + \left(\frac{\Delta Sa}{R}\right) - \left(\frac{\Delta Ha}{RT}\right) \quad (6) 1n\left(\frac{CR}{T}\right)$$

Where N is the Avogadro's Number (6.02252 x 10^{23} mol^{-1}) and h is the Plank's constant (6.626176 x 10^{34} Js) while other parameters have their usual definition. A plot of $1n(\frac{C_R}{T})$ versus $1/T$ gave a straight line with a slope equal to $(\frac{-\Delta H_a}{2.303R})$ and an intercept of $1n(\frac{R}{Nh} + \frac{\Delta S_a}{R})$ from which the values of ΔS_a and ΔH_a were calculated and presented in table 1.

The large positive value of ΔH_a and the negative value of ΔS_a recorded in table indicate that the adsorption of inhibitors on the surface of low carbon steel is endothermic in nature also revealed spontaneity and the feasibility of the reaction. This result conforms to that of [28]. It can also be seen from the table that E_a and ΔH_a values vary in the same way with inhibitor concentration. This result verifies the known thermodynamic relation between E_a , ΔH_a and $\Delta G^o{}_a$, and is in agreement with works of [32].

Table 2 Adsorption Isotherms for the Adsorption of *Honeycomb propolis* extract on Mild Steel Surface at 303-333K.

Isotherm	Slope	K_{ads}	R^2
Langmuir			
303K	1.056	0.947	0.991
313K	0.952	1.051	0.977
323K	1.007	0.993	0.943
333K	0.937	1.067	0.990
Temkin			
303K	0.363	2.752	0.967
313K	0.507	1.972	0.947
323K	0.504	1.984	0.922
333K	0.561	1.782	0.988
Freundlich			
303K	0.095	10.504	0.941
313K	0.230	4.342	0.990
323K	0.345	2.897	0.991
333K	0.485	2.062	0.997
FloryHuggins			
303K	0.990	1.010	0.825
313K	0.520	1.923	0.821
323K	0.722	1.384	0.936
333K	0.768	1.301	0.976

Table 2 shows parameters of various adsorption isotherm for the adsorption *Honeycomb propolis* extract on mild steel surface at 303-333K. the intercepts, slope, R^2 and K_{ads} values were obtained from transition state plots. the adsorption characteristics of Honeycomb propolis extract on the metal surface was found to best fit the Freundlich adsorption model taking into cognizance that the plot gave linear slopes with regression coefficients, R^2 of these lines were nearly unity, meaning that each inhibitor molecule occupies one active site on the metal surface (strong adsorption of inhibitors) [28,34]. And the negative value of $\Delta G^o{}_{ads}$ indicated spontaneity of the reaction and feasibility of the adsorption process for the mild by the inhibitor *Honeycomb propolis* extract. Knowing that the natural extract contains an infinity of chemical compounds at different concentrations, the higher protection of mild steel in HCl solution is due by a competitive action of several molecules and ions [36-37]. Then, the inhibitory effect occurs via an intermolecular synergistic effect of several molecules / ions of extract [37-39].

3.3 FTIR Spectrophotometry Analysis

To further support the adsorption behaviour of the inhibitor on the surface of mild steel, IR spectroscopy was employed. Figure 4a represent the IR spectra of *Honeycomb propolis* extract and

Figure 4b shows the IR the spectra of the corrosion product when ethanol extract of *Honeycomb propolis* was used as an inhibitor. from the results obtained, shows that the O-H stretch at 3346 cm^{-1} was disappeared and the band at 2921 cm^{-1} and 2854 cm^{-1} shifted to 2918 cm^{-1} and 2851 cm^{-1} Respectively. the C=O stretch at 1655 cm^{-1}, 2117 cm^{-1} due to -C=C- 1175 cm^{-1} due to C-O-C were all disappeared. However, shifts were observed from 1380 cm^{-1} to 1376 cm^{-1} and from 1462 cm^{-1} to 1451 cm^{-1}, also, from 1655 cm^{-1} to 1622 cm^{-1} assigned to C=O, likewise, 2117 cm^{-1} shifted to 2110 cm^{-1} due bond in –C=C-Other functional groups were missing and some appeared in the spectrum of the corrosion product as stated above, suggesting that these bond frequencies might have been used for bonding between the vacant d-orbital of Fe and the inhibitor and the result conforms to the [40,41].

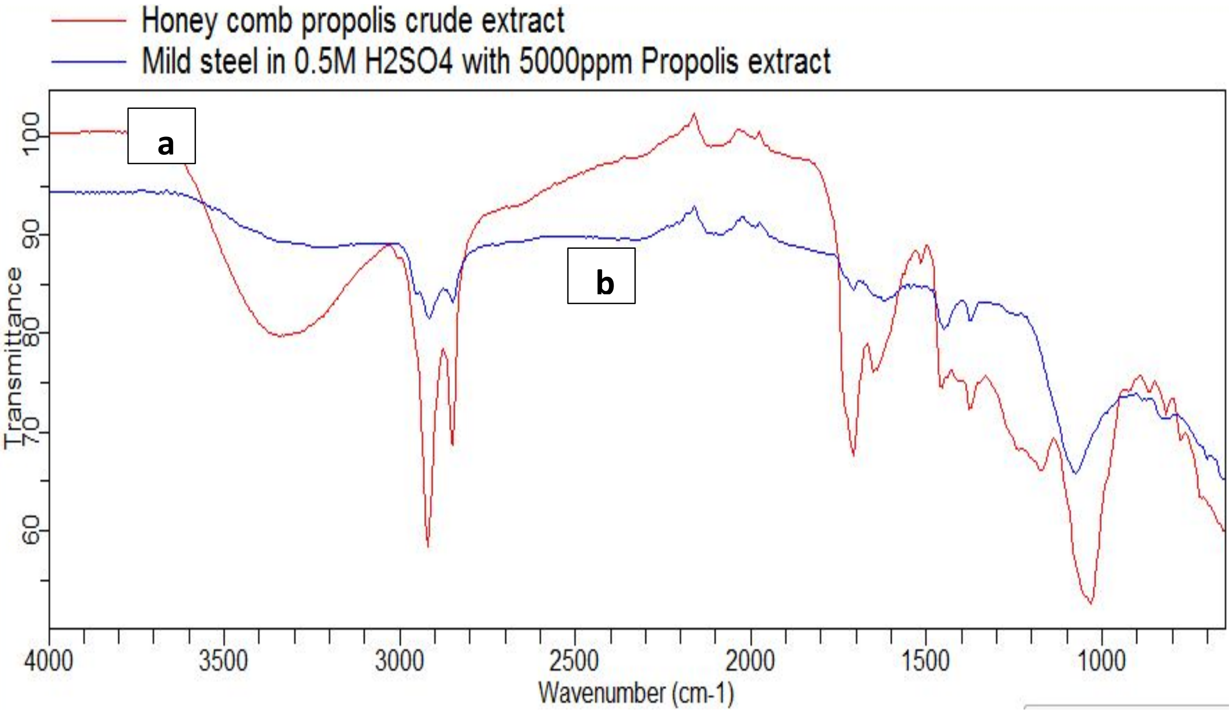

Figure 4a represent the IR spectra of *Honeycomb propolis* extract and Figure 4b shows the IR the spectra of the corrosion product when ethanol extract of *Honeycomb propolis*

3.4 UV-Visible Spectroscopy Analysis

Figure 5a-b illustrates the UV-Vis spectra for *Honeycomb propolis* extract (a) and the solution containing corrosion product of mild steel sample immersed in the extract (b). A careful investigation of Figure 5 revealed that both spectral were similar in appearance but having different adsorption coefficient, the e shift of band from 219.98nm to 217.08nm, 249.14nm to 248.47nm, 286.78nm to 279.93nm, 309.68nm to 308.19nm and appearance of new bands like 327.21nm, 336.09nm and 344.94nm in the shape of the corrosion products spectra indicate the formation of a complex between two species in solution [42]. On the basis of this fact, it can be concluded that the phytochemical components present in the *Honeycomb propolis* extract were adsorbed on the mild steel surface.

3.5. SEM Scanning Electron Microscopy

The SEM micrograph image in Figure 6a showed that the mild steel specimen immersed in inhibited solution experience minimal if any visible damages and it has a fairly smooth surface. This provided proof of corrosion inhibition effectiveness of *HoneyComb propolis* extract against the mild steel corrosion in 0.5M H_2SO_4 solution. In order words, it has far better surface condition. Similarly, presented, in Fig 6b, is a SEM micrograph of the mild steel surface immersed in the uninhibited 0.5M H_2SO_4 solution.

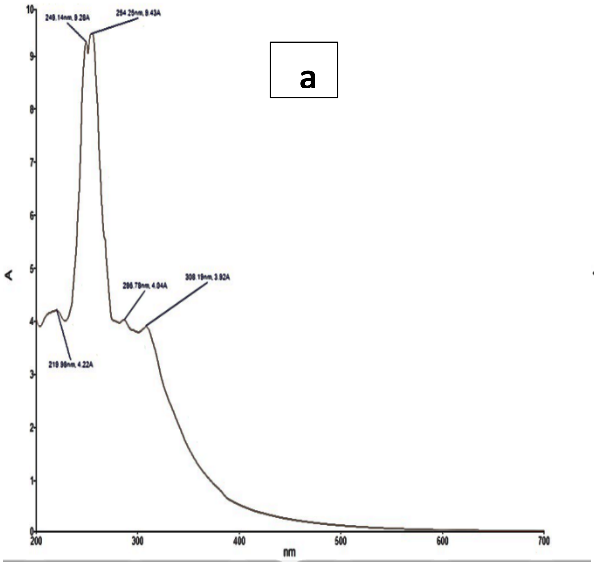

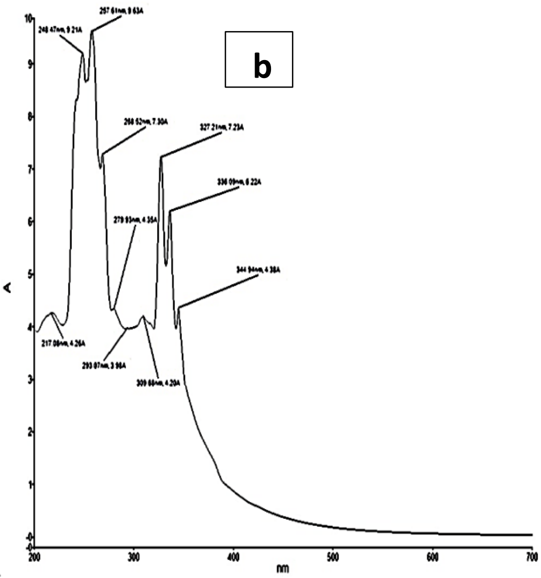

Figure 5a: UV-Visible spectrum of *Honeycomb propolis* crude extract

Figure 5b: UV-Visible spectrum of corrodent solution containing 5000ppm *Honeycomb propolis* Extract

Unlike the micrograph image in Fig. 6a, the micrograph image in Figure 6b as can be seen possesses a very rough surface full of numerous corrosion cracks and products and in addition to those, also consists of many pits and corrosion cavities from the corrosion attacks. These experimental results presented strong evidence that there was formation of a barrier thin layer by the inhibitor molecule which provided the effective protection for mild steel surface against the aggressive attacks from the corrosive acidic media. Similar research works have been reported by many researchers [2,43-45].

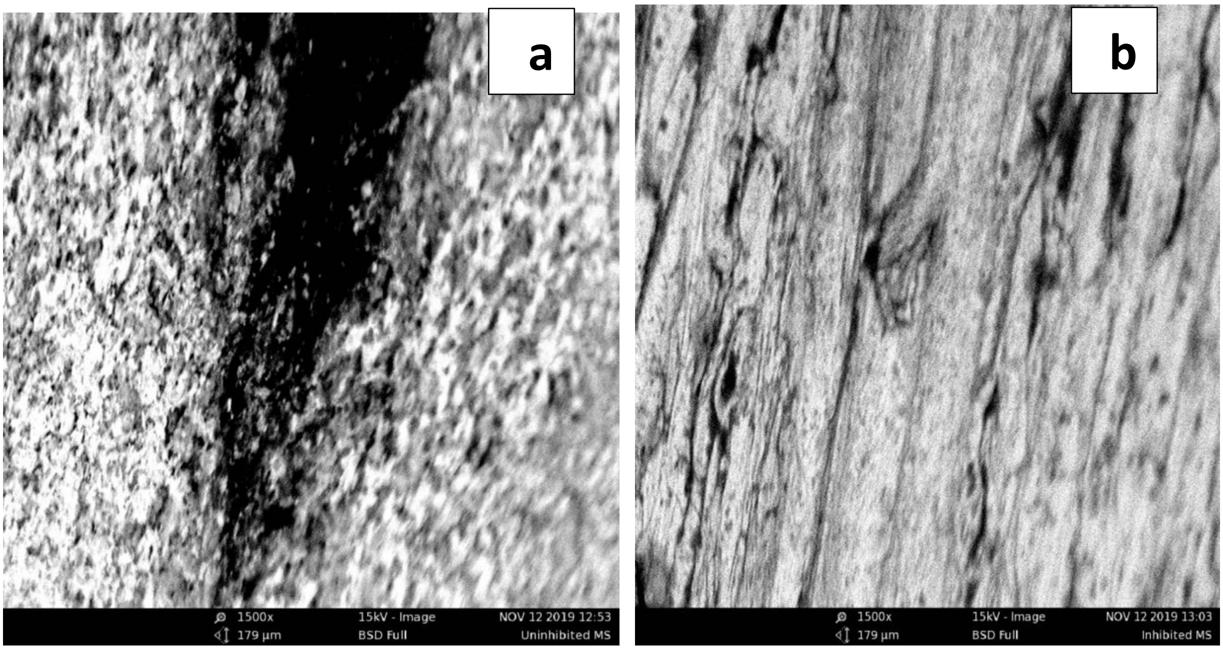

Figure 6. (a)SEM micrograph of mild steel immersed in 0.5M H_2SO_4 solution (A); (b)SEM micrograph of mild steel immersed in 0.5M H_2SO_4 containing 5000ppm of *Honeycomb propolis* extract for 4 hours

3.6. Gas Chromatography Spectrophotometry

The chemical composition detected by GC-MS of the ethanol extract of honeycomb propolis shows twenty-six compounds as shown in Figure 7 and Table 3. The main constituents are 9,12-Octadecadienal (27.59%), 9-Octadecenoic acid, ethyl ester(19.02%), n-Hexadecanoic acid(10.06%), Hexadecanoic acid, ethyl ester(10.64%), Linoleic acid ethyl ester(9.92%) and Ethyl .alpha.-d-glucopyranoside(3.08%). From which the quantum chemical calculation and molecular dynamics simulation was also carried out to confirm the inhibition activity of *honeyComb propolis* extract.

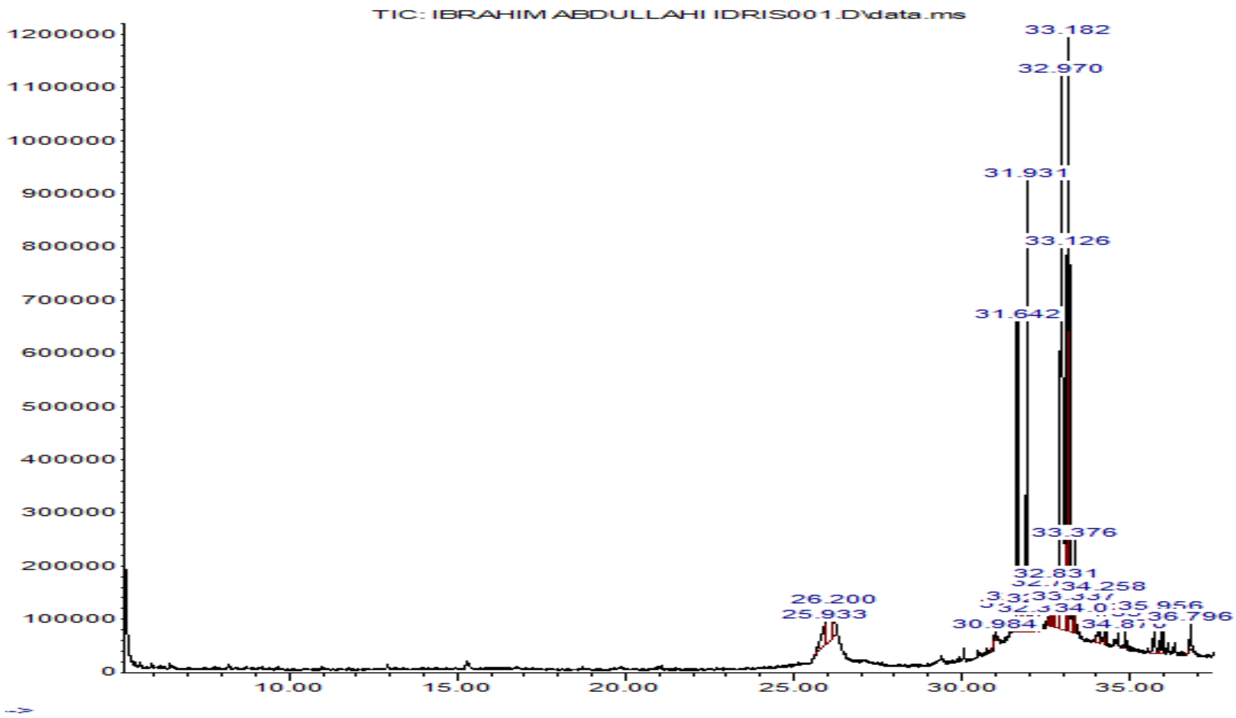

Figure 7. GC-MS chromatogram of *Honeycomb propolis* extract

3.7. Quantum Chemical Calculations

The quantum chemical calculations were carried out with Material Studio (version 8.0).The geometry optimization of the molecules was performed using DFT (Spartan 14) at Becke three Yarg and Parr with 6-311G^{++}(d, p) basis set as B3LYP/6- 311G^{++}(d, p) [2,46-49]. The quantum chemical assessments were used to search for good quantum chemical descriptors to be incorporated with the inhibitive performance of the molecule. E_{HOMO}, E_{LUMO}, ΔE_{gap}, electronegativity (X), ionization energy (I), electron affinity (A), hardness (ɳ), softness (S), fractions of electrons (ΔN), global electrophilicity index (φ), The affinity (A), ionization energy (I), energy gap (ΔE_{gap}) and electronegativity (X) were calculated according to Koopman's theory [2,48] using equation 10-17 below:

$A = -E_{LUMO}$ (8)

$I = -E_{HUMO}$ (9)

$\Delta E_{gap} = -E_{LUMO} - E_{HUMO}$ (10)

$X = \frac{(I+A)}{2}$ (11)

While hardness (η) and softness (S) were obtained using equations (12) and (13) respectively

$\eta = \frac{(I-A)}{2}$ (12)

$S = \frac{1}{\eta} \ or \ \frac{2}{I-A}$ (13)

The fraction of electrons transferred (ΔN) from the inhibitor to metal were calculated using equation (14) [50,51]

$$\Delta N = \frac{X_{Fe} - X_{inh}}{[2(\eta_{Fe}+\eta_{inh})]} \quad (14)$$

Where a theoretical value of X_{Fe} ≈7 eV/mol (0.257au) is taken for iron, and η_{Fe} =0eV/mol (0.000au) for the computation of number of transferred electrons [52] were used.

The global electrophilicity index (φ), which measures the electrophilic power of a molecule, according [51,53] is defined by equation (15).

$$\varphi = \frac{X_{inh}^2}{4\eta_{inh}} \quad (15)$$

Table 3 Chemical composition for the ethanol extract of Honeycomb propalis

PK	RT	Area Pct	Library/ID	Quality
1	25.9335	2.2757	Beta.-D-Ribopyranoside, methyl	32
2	26.1028	3.0805	Ethyl .alpha.-d-glucopyranoside	56
3	26.1231	0.5083	Ethyl .alpha.-d-glucopyranoside	56
4	26.2	1.8783	Ethyl .alpha.-d-glucopyranoside	72
5	30.9842	0.1486	n-Hexadecanoic acid	55
6	31.6424	10.0627	n-Hexadecanoic acid	99
7	31.7768	0.3368	n-Hexadecanoic acid	52
8	31.931	10.6395	Hexadecanoic acid, ethyl ester	97
9	32.0377	1.1566	Carbonic acid, but-3-en-1-yl dodecyl ester	49
10	32.3187	0.2072	E,E-10,12-Hexadecadien-1-ol acetate	84
11	32.6307	0.6281	Cyclopentaneundecanoic acid	43
12	32.6775	0.8261	Oleic Acid	76
13	32.7077	0.5728	9-Oxabicyclo[6.1.0]nonane	64
14	32.7416	1.2916	Oleic Acid	90
15	32.8306	1.4112	9,12-Octadecadienal	53
16	32.9704	27.5948	9,12-Octadecadienal	90
17	33.1263	9.9207	Linoleic acid ethyl ester	97
18	33.1824	19.0176	9-Octadecenoic acid, ethyl ester	93
19	33.3365	0.7253	Oleic Acid	42
20	33.3762	1.7914	Octadecanoic acid, ethyl ester	97
21	34.0561	1.0281	Erucic acid	68
22	34.2583	1.1685	Tricosane	89
23	34.8696	0.4472	7-Octenoic acid, ethyl ester	35
24	35.7086	1.2385	Pentacos-1-ene	96
25	35.9562	1.2064	Eicosane	93
26	36.7959	0.8374	Propionic acid, 3-(2-methylcyclohexyl)-, ethyl ester	25

Quantum chemical calculations have been used to quantify the inhibition efficiency of the active component inhibitors of *Honeycomb propolis* extract. Table 4, represent the quantum chemical calculation parameters obtained by DFT method with quantum chemical software, Spartan 14. The energy of the E_{HOMO} orbital (E_{HOMO}) is a measure of relative tendency of a molecule to donate electrons to an electron accepting specie [54-59]. Linoleic acid ethyl ester (LEE) has the highest value of E_{HOMO} energy (E_{HOMO}), which implies highest tendency to donate electrons to an electron deficient site. This suggests that LEE has the highest tendency to adsorb onto mild steel surface. The E_{LUMO} energy (E_{LUMO}) is a measure of the tendency of a molecule to accept electron(s) from electron rich specie. Molecules with low E_{LUMO} values tend to accept electrons easily [58-59]. Though, 9,12-Octadecadienal (OCD) has a relatively low E_{HOMO}, its very low E_{LUMO} offers it a better chance of accepting charges in a favourable retro-donation/ back-bonding formation during donor-acceptor interactions with the metal. The frontier molecular orbitals energy gap, ΔE ($\Delta E = E_{LUMO} = E_{HOMO}$) is often used to characterize the chemical reactivity and kinetic stability of molecules [57] posited that molecules with large value of ΔE are highly stable (i.e., they have low reactivity to chemical species) whilst molecules with small value of ΔE have a high reactivity.

Table 4. Quantum Chemical descriptors and their values

Descriptors	n-Hexadecanoi acid	9,12-Octadecadienal	Linoleic acid ethyl ester	Ethyl .alpha.-d-glucopyranoside	9-Octadecenoic acid, ethyl ester
E_{HOMO} (ev)	-7.38	-6.38	-6.30	-6.65	-6.34
E_{LUMO} (ev)	0.33	-0.57	0.48	1.18	0.50
ΔE_{gap}(ev)	7.71	5.81	6.78	7.83	6.84
χ (ev)	3.53	3.46	2.91	2.74	2.92
I (ev)	7.38	6.38	6.30	6.65	6.34
A (ev)	-0.33	0.57	0.48	-1.18	-0.50
S (ev)	0.26	0.34	0.29	0.26	0.29
η (ev)	3.86	2.91	3.39	3.92	3.42
μ (debye)	1.40	3.07	2.05	4.30	1.67
ΔN (ev)	0.46	0.61	0.60	0.55	0.59
φ(ev)	0.81	1.04	0.62	0.48	0.62
Weight	256.43	264.45	308.51	208.21	310.52

The results reported in Table 4, show OCD has the smallest ΔE value and therefore corresponds to the most reactive compound.To predict the direction of a corrosion inhibition process, the important electronic parameter fitted to achieve this purpose is the dipole moment (μ). The dipole moment provides information on the polarity (hydrophobicity) in a bond of a molecule and therefore the electronic distribution in the molecule [2]. It is generally believed that better inhibition results from the adsorption of high polar compounds possessing high dipole moment on the metal [43,60]. In the present calculation, Ethyl .alpha.-d-glucopyranoside(EADG) has the highest dipole moment 4.30 debye. The higher value of the dipole moment of the EADG molecule confirms its high inhibition efficiency property. This higher inhibition property may be attributed to the large size of the phytochemical constituent of the plant extract covering a wider area of the metal surface thereby minimizing the corrosion rate [2,41,43]. Absolute hardness and softness are important properties to measure the molecular stability and reactivity. In this concept, a hard molecule is said to have a large ΔE value, while a soft molecule has a small ΔE value. Adsorption usually occurs at the region of the molecule where σ has the highest value (6). The order across structures in the σ values as reported in Table 4 is such that OCD>LEE ≈ ODEE>NHC≈ EADG, which also suggests that ODC is the most reactive compound.

The descriptor, ΔN, shows inhibition effect that donates the electrons fraction transferred which shows the ability of the molecule to donate electrons and therefore to be adsorbed on the metal surface with ease. If the value of Δ*N* is less than 3.6 eV, then the inhibition efficiency increases by increasing electron-donating ability of the inhibitor to donate electrons to the metal surface. Therefor from the table4, the positive ΔN value shows that the inhibitor molecule adsorption onto the metal surface proceeds through electron donating mechanism, and therefore, it is an electron-donation specie [2,60]. The positive value of ΔN shows that the molecule acts as an electron donor, while a negative value of ΔN indicate that the molecule have activity as electron acceptors. An electrophilicity value provides information on the nucleophilic or elecrophilic nature of a molecule. A high electrophilic value explains that the molecule has a high potential to act as an electrophile while a low value of electrophilicity informs that the molecule has a high tendency to act as a nucleophile. A good, more reactive, nuceophile is characterized by lower value of φ and conversely a good electrophile is characterized by a high value of φ [60]. From Table 4, it is clear that the value of φ is low therefore the molecules has lower capacity to accept electron. The molecular structure, Optimized structure, energy of HUMO and LUMO for n-Hexadecanoic Acid, 9,12-Octadecadienal, Linoleic acid ethyl ester, Ethyl .alpha.-d-glucopyranoside, 9-Octadecenoic acid, ethyl ester are represented in Figure 8.1-8.5 a, bc and d respectively.

Molecular Structure of n-Hexadecanoic Acid	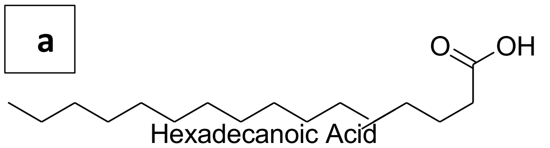
Optimized Structure of n-Hexadecanoic Acid using DFT at the B3LYP/6-311G^{++} basis set level	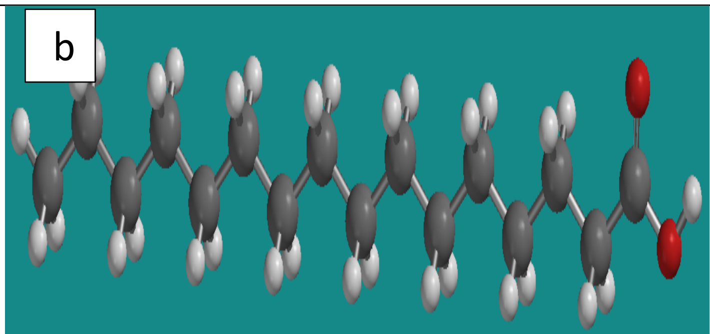
The highest occupied molecular orbital (HOMO) of n-Hexadecanoic Acid using DFT at the B3LYP/6-311G^{++} basis set level	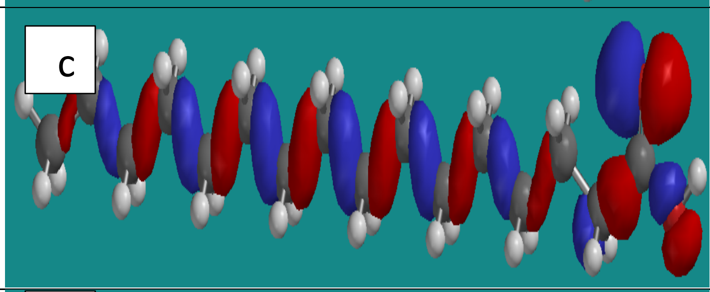
Lowest unoccupied molecular orbital (LUMO) of n-Hexadecanoic Acid using DFT at the B3LYP/6-311G^{++} basis set level	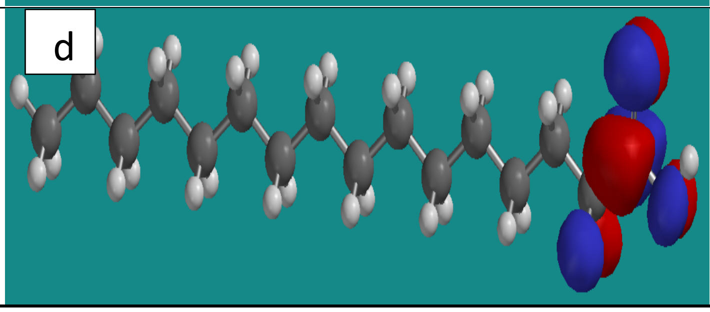

Figure 8.1 a,b, c and d: Molecular Studies and Optimized Structure n-Hexadecanoic Acid

Molecular Structure of 9,12-Octadecadienal	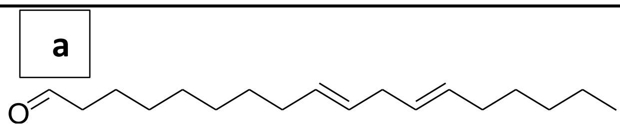
Optimized Structure of 9,12-Octadecadienal using DFT at the B3LYP/6-311G^{++} basis set level	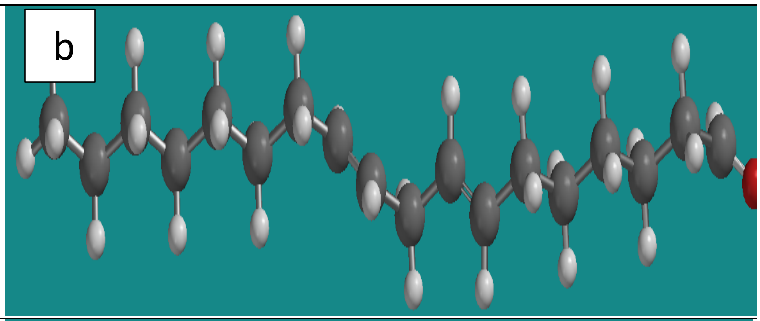
The highest occupied molecular orbital (HOMO) Of 9,12-Octadecadienal using DFT at the B3LYP/6-311G^{++} basis set level	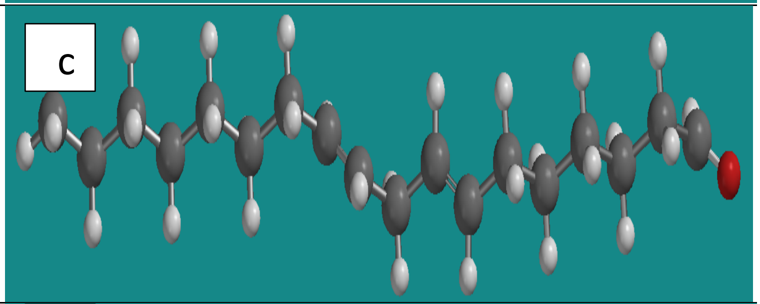
Lowest unoccupied molecular orbital (LUMO) of 9,12-Octadecadienalusing DFT at the B3LYP/6-311G^{++} basis set level	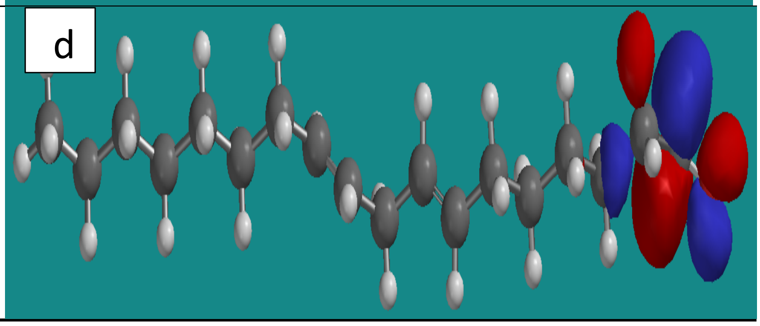

Figure 8.2 a,b, c and d: Molecular Studies and Optimized Structure of 9,12-Octadecadienal.

Molecular Structure of Linoleic acid ethyl ester	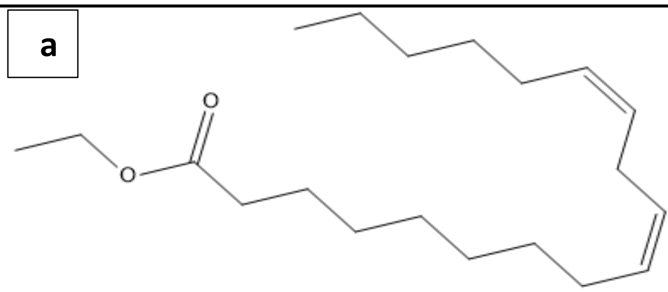
Optimized Structure of Linoleic acid ethyl ester using DFT at the B3LYP/6-311G^{++} basis set level	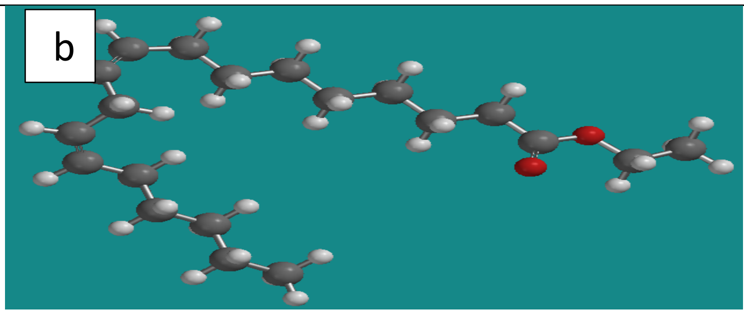

The highest occupied molecular orbital (HOMO) Of Linoleic acid ethyl ester using DFT at the B3LYP/6-311G^{++} basis set level	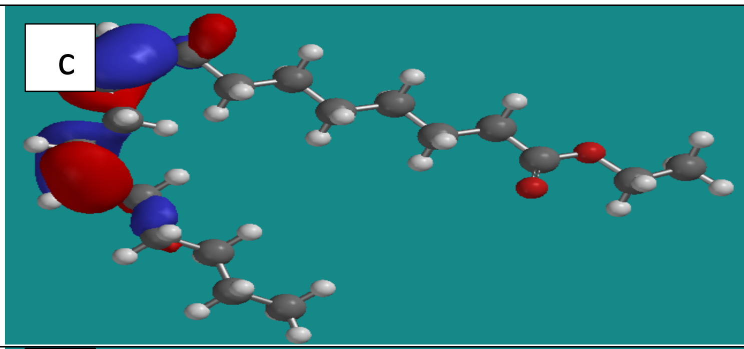
Lowest unoccupied molecular orbital (LUMO) of Linoleic acid ethyl ester using DFT at the B3LYP/6-311G^{++} basis set level	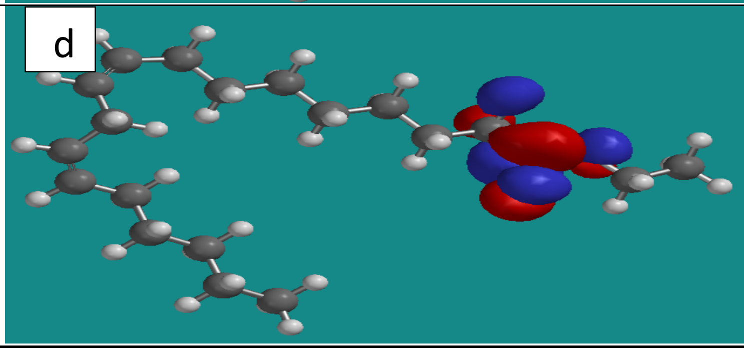

Figure 8.3 a,b, c and d: Molecular Studies and Optimized Structure of Linoleic acid ethyl ester.

Molecular Structure of Ethyl.alpha.-d-glucopyranoside	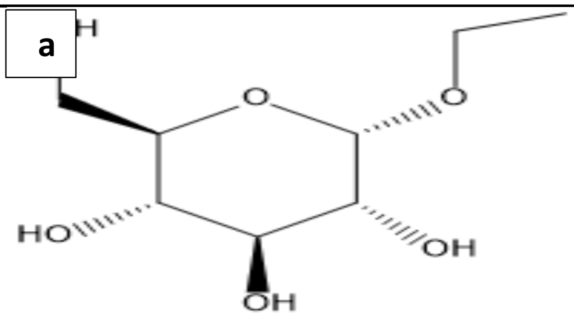
Optimized Structure of Ethyl .alpha.-d-glucopyranoside using DFT at the B3LYP/6-311G^{++} basis set level	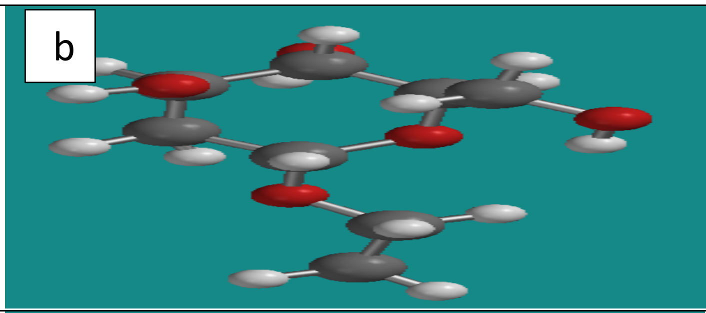
The highest occupied molecular orbital (HOMO) of Ethyl .alpha.-d-glucopyranoside using DFT at the B3LYP/6-311G^{++} basis set level	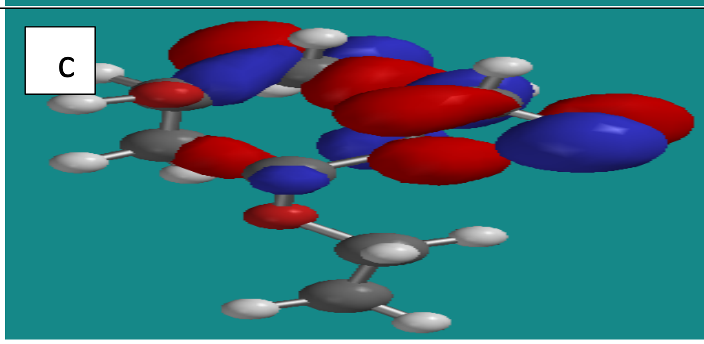

Lowest unoccupied molecular orbital (LUMO) of Ethyl .alpha.-d-glucopyranoside using DFT at the B3LYP/6-311G^{++} basis set level	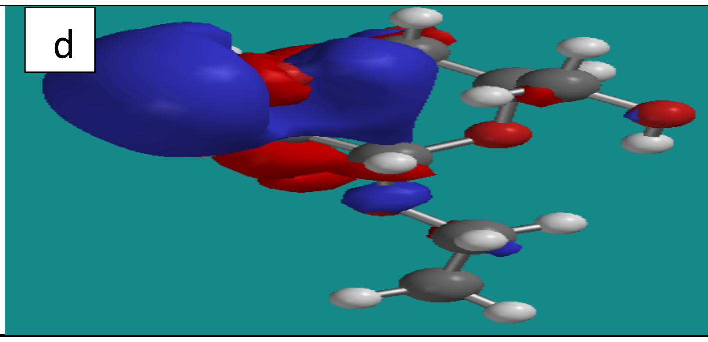

Figure 8.4 a, b, c and d**:** Molecular Studies and Optimized Structure of Ethyl.alpha.-d-glucopyranoside.

Molecular Structure of 9-Octadecenoic acid, ethyl ester	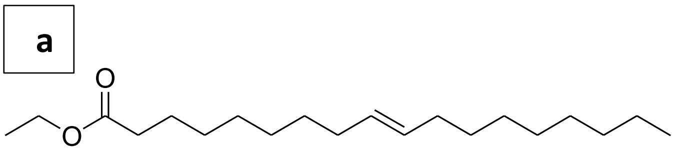
Optimized Structure of 9-Octadecenoic acid, ethyl ester using DFT at the B3LYP/6-311G^{++} basis set level	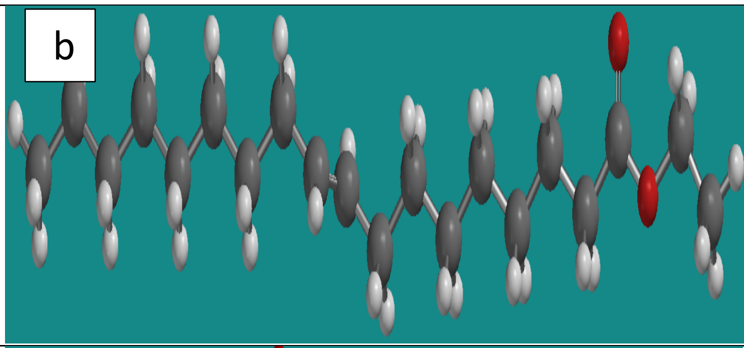
The highest occupied molecular orbital (HOMO) 9-Octadecenoic acid, ethyl ester using DFT at the B3LYP/6-311G^{++} basis set level	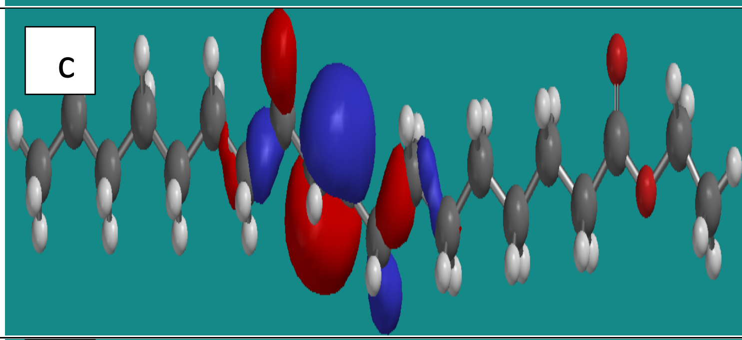
Lowest unoccupied molecular orbital (LUMO) of 9-Octadecenoic acid, ethyl ester using DFT at the B3LYP/6-311G^{++} basis set level	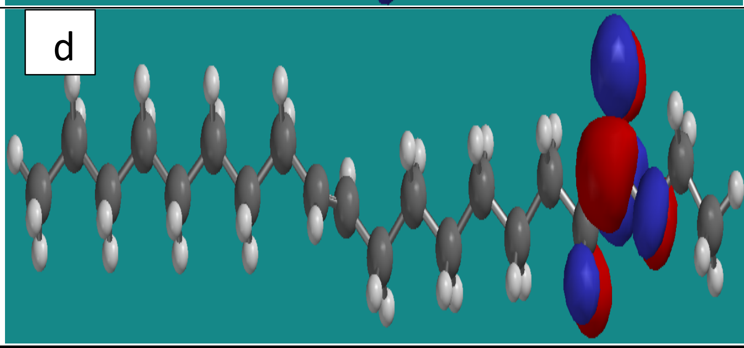

Figure 8.5 a,b, c and d: Molecular Studies and Optimized Structure of 9-Octadecenoic acid, ethyl ester.

4.2 Molecular Dynamic Simulations

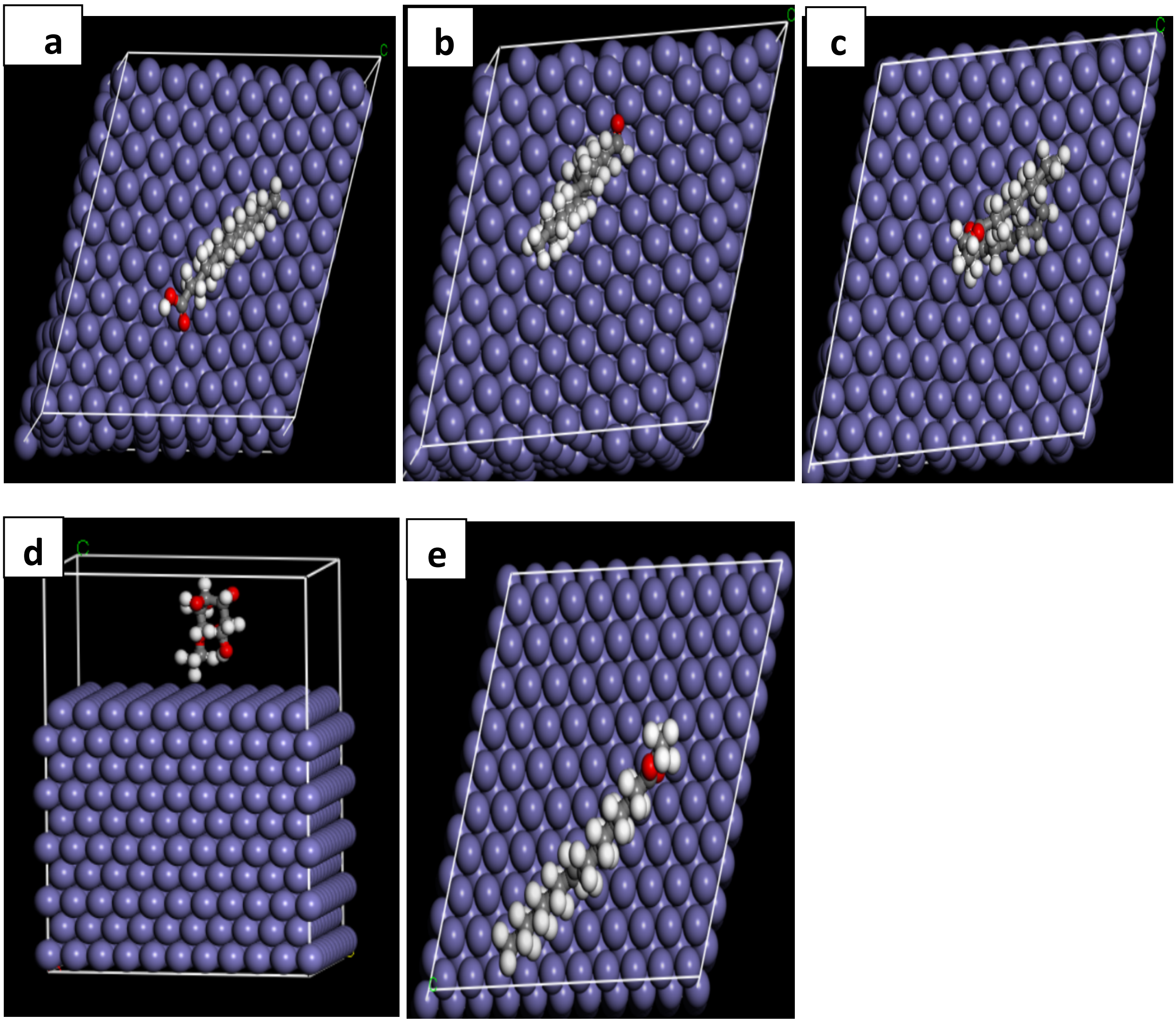

Figure 9: side view snap shot of adsorbed (a) NHC (b) ODC (c) LEE d) EADG (e) ODEE molecule onto mild steel (1 1 0) surface with preferred binding site

The molecular dynamics simulation was introduced to analyse the adsorption behaviour (pattern, strength and properties) of the molecules on the Fe (110) surface [62]. For instance, the fluctuations of temperature and energy should be confined to 5–10% [62]. The temperature fluctuates in a range of (298± 20) K and the fluctuation of energy is less than 0.5%, indicating that the system has reached an equilibrium state. Figure 9 shows representative of the snapshots of the lowest energy adsorption configuration of the molecules onto Fe (110) surface from the stimulations. The molecule maintain a flat-lying adsorption orientation on the surface of the metal thereby maximize its contact with the studied surface as the system reached equilibrium. The adsorption has been observed to occur through moieties containing the aromatic rings π- electron and the hetroatom (O) in the molecules with metal surface. This result conforms to the finding of [60] the binding and interaction energies of the adsorbed inhibitor molecule were approximated as the simulation system reached their equilibrium state. The most stable adsorption configuration of the molecules onto Fe (110) are presented in Figures 9a-e: The adsorption has been observed to occur through O-atom as well as -bond on the ring. The assessment of the quantitative interaction between the inhibitor molecule and Fe (110) surface was accomplished by evaluating the interaction energy ($E_{interaction}$). Thus, the binding and interaction energies of the adsorbed inhibitor molecule were approximated as the simulation system reached their equilibrium state [2,43]. Similarly, the distribution of interaction and binding energies of the inhibitor molecule on Fe (110) are presented in Table 5 which suggests that n-Hexadecanoic acid has the strongest interaction with Fe(110) surface.The very large negative values of the interaction energy of n-Hexadecanoic acid described the spontaneity of the adsorption process and its strong adsorption behaviour on the studied surfaces. Also, it can be seen from Table 5 that the binding energies of the adsorption of inhibitors on Fe (110) surface equally has a large positive value indicating that the adsorbed inhibitor molecule possessed high stability on the studied surface [2,43,62-63]. This result quite agreed with experimental and quantum chemical calculations studies which revealed that the inhibitor molecule possesses a better corrosion inhibition performance.

Table 5. Interaction and Binding energies from molecular dynamics simulations

System	$E_{interaction}$(kcalmol^{-1})	$E_{binding}$(kcalmol^{-1})
Fe + n-Hexadecanoic acid	-27.023	27.023
Fe + 9,12-Octadecadienal	-15.09	15.09
Fe + Linoleic acid ethyl ester	-19.331	19.331
Fe + Ethyl .alpha.-d-glucopyranoside	-14.915	14.915
Fe + 9-Octadecenoic acid, ethyl ester	-10.099	10.099

Conclusion

This result shows that the ethanol *Honeycomb propolis* extract has good efficiency towards corrosion inhibition of mild steel and the inhibition efficiency increases with increase in the concentration of inhibitor. The effect of temperature indicates that the inhibition efficiency decreased with rise in temperature. The activation energy (E_{ads}) was found to be higher for inhibited acid solutions than for uninhibited acid solution showing the temperature dependence of inhibition efficiency. The positive value of ΔH_{ads} and negative values of ΔS_{ads} indicates endothermic reaction which proceeds with decreases in randomness at the metal-electrolyte interface. The results from the FTIR, UV-visible spectra confirmed that the process of adsorption of the extract on the metal surface was physisorption. The SEM micrograghs demonstrated that the metal surface becomes smooth in the presence of *Honeycomb propolis* extract which indicate the presence of protective layers over the metal surface. GC-MS revealed that the main phytochemical component responsible for corrosion inhibition in *Honeycomb propolis* extract is reach in several constituent such as 9,12-octadecadienal (27.59%), 9-octadecenoic acid, ethyl ester (19.02%), Hexadecanoic acid, ethyl ester (10.64%) and Linoleic acid ethyl ester (9.92%) providing evidence for the corrosion inhibitory effect of the inhibitors. From quantum chemical calculation, it has been confirmed that the molecules have better inhibition efficiency because it has high E_{HOMO} value, lower E_{LUMO} value and low energy gap values indicating its high ability of offering and accepting electrons and hence, could have better performance as corrosion inhibitor. Molecular Dynamics simulation showed that the inhibitor molecules have the potential to be strongly adsorbed on mild steel surface with great stability.

Acknowledgement
The authors acknowledged Mechanical Engineering Department Bayero University Kano and Central Laborotory Ahmadu Bello University Zaria for the characterization of metal and inhibitor respectively.

Disclosure statement: *Conflict of Interest:* In this study no conflict of interest
*Compliance with Ethical Standards***:** The article doesn't contain a study involving human or animal samples.

References

[1] J.C. Philip. Survey of Industrial Chemistry (Wiley, New York, 1987), 45–57

[2] B.K. Subrahmanya, H. Lgaz, R. Salghi, R Chaouiki, A., Shubhalaxmi, and S.Jodeh, Pyrazoline derivatives as possible corrosion inhibitors for mild steel in acidic media: A combined experimental and theoretical approach. *Cogent Engineering (Material Engineering and Research Article)* 5 (2018) 1441585.

[3] T. Laabaissi, H. Lgaz, H. Oudda, F. Benhiba, H. Zarrok, A. Zarrouk, and R. Touir Comparative study of corrosion inhibition effect of benzodiazepine derivative on the carbon steel surface in 2.0 M H_3PO_4 and 1.0 M HCl mediums: Electrochemical, theoretical and Monte Carlo simulations studies. *Journal of Materials and Environmental Science*, 8(3) (2017)1054-1067.

[4] R.Salghi, S. Jodeh, E.E Ebenso, H. Lgaz, D. Ben-Hmamou, I.H. Ali, and N. Benchat, N. (6-phenylpyridazin-3(2H) one as New corrosion inhibitor for C38 steel in 1 M HCl. *International Journal of Electrochemical Science,* 12(4) (2017) 3309–3322

[5] B. E. A. Rani, and B. B. J. Basu, Green inhibitors for corrosion protection of metals and alloys: An overview. *International Journal of Corrosion.*, (15) (2012a) 380217.

[6] J. Aljourani, K. Raeissi, and M. Golozar, Benzimidazole and its derivativesas corrosion inhibitors for mild steel in 1 M HCl solution. *Corrosion Science,* 51 (8) (2009) 1836–1843.

[7] E. Machnikova, K.H. Whitmire, and N. Hackerman, Corrosion inhibition of carbon steel in hydrochloric acid by furan derivatives. *Electrochimica Acta, 53*(20): (2008) 6024-6032.

[8] Y. El Aoufir, J. Sebhaoui, H. Lgaz, Y. El Bakri, A. Zarrouk, F. Bentiss, and H. Oudda, Corrosion inhibition of carbon steel in 1 M HCl by 1,5-benzodiazepine derivative: Experimental and molecular modeling studies. *Journal ofMaterials and Environmental Science, 8*(6) (2017) 2161–2173.

[9] R. Kumar, S. Chahal, S. Kumar, S. Lata, H. Lgaz, R. Salghi, and S. Jodeh, Corrosion inhibition performance of chromone-3-acrylic acid derivatives for low alloy steel with theoretical modeling and experimental aspects. *Journal of Molecule Liquids,* 243 (2017)439–450.

[10] H. Lgaz, R. Salghi, S. Jodeh, and B. Hammouti, Effect of clozapine on inhibition of mild steel corrosion in 1.0 M HCl medium. *Journal of Molecular Liquids,* 225 (2017)271–280.

[11] M. Messali, H. Lgaz, H., Dassanayake, R., Salghi, R., Jodeh, S., Abidi, N., and Hamed O. Guar gum as efficient nontoxic inhibitor of carbon steel corrosion in phosphoric acid medium: Electrochemical, surface, DFT and MD simulations studies. *Journal of Molecular Structure,* 1145 (2017) 43–54.

[12] M.S. Al-Otaibi, A.M. Al-Mayouf, M. Khan, A. A, Mousa, S. A. Al-Mazroa, and H. Z. Alkhathlan "Corrosion inhibitory action of some plant extracts on the corrosion of mild steel in acidic media," *Arabian Journal of Chemistry*, 5(1) (2012) 1-7.

[13] I. B. Obot, N. O. Obi-Egbedi, and S. A. Umoren, "Antifungal drugs as corrosion inhibitors for aluminium in 0.1 M HCl," *Journal Corrosion Science,* 51(8) (2009) 1868-1875.

[14] A. Yıldırım, and M. Çetin, "Synthesis and evaluation of new long alkyl side chain acetamide, isoxazolidine and isoxazoline derivatives as corrosion inhibitors, *Corrosion Science*, 50 (1) (2008) 155-165.

[15] A. H. Banksnota, Y. Tezuka, and S. H. Kadota, Recent progress in pharmacological research of propolis, *Phytother. Res.* 15 (2001) 561–571.

[16]V. L. Singleton, R. Orthofer, and R. M, Lamuela-Raventos, Analysis of total phenols and other oxidation substrates and antioxidants by means of Folin-Ciocalteu reagent, Methods Enzymol. 299 (1999) 152–178.

[17] C. A. Loto, T. R. Loto, and I.P.A. Popoola, "Corrosion and Plant Extracts Inhibition of Mild Steel in HCL".*International Journal of The Physical Sciences*, 6(15) (2011) 3616-3623.

[18] K. F. Khaled, (2008). "New Synthesized guanidine derivative as a green corrosionfor mild steel in acidic solutions". *International Journal of Plant, Animal and Environment* (3) (Year) 462-475.

[19] Gapal, K., Sinha, A. K., Choudhary, P.K., Robetson, A. and Kumar R. Effect of replacement of groundnut cake with niger seed cake n serum biochemical profile and protein efficiency ratio in broiler chicken. *Journal of Interaacademicia*. 19 (1) (2015) 82-87.

[20] A. S. Kadhim. Inhibition of Aluminium (AA3105) Corrosion in HCl by Acetamide and Thiourea. *Nigerian Journal of Corrosion.* 17(10) (2016) 441-452.

[21] O. A. Omotosho, (2016). Inhibition Evaluation of Chemical and Plant Extracts on the Corrosion of Metallic Alloys in Acidic Environment. *An Unpublished PhD. Thesis, Covenant University of Nigeria.* (2016)

[22] B. Usman, and I. Jimoh, Corrosion Inhibition Effect of Ethanol Extract of *Acacia nilotica* Leaves on Mild Steel in Acid Medium. *Portugaliae Electrochimica Acta,* 39 (2) (2021) 105-128.

[23] H. Derfouf, Y. Harek, and L. Larabi, Corrosion Inhibition of Artemisia alba Extract on Carbon Steel In Hydrochloric Acid. International *Journal of Environmental Engineering*. 1(2) (2014) 234-249.

[24] U. J. Ekpe., B. I Ita, and A. E. Bassey, The Study of Corrosion of Aluminium Manganese Alloy in Alkaline Medium by *Carica papaya* Leaves Extract. *Global Journal of Pure and Applied Sciences.* 31(5) (2004) 49-59

[25] I. A. Onen, Kinetic Studies of Selected Corrosion Inhibitors of Aluminium in Mild Steel in Acidic Medium. *An Unpublished PhD. Thesis Submitted to the Dept. of Chemisty, Natural Science, Uni Jos*. (2010).

[26] Y. El Bakri, M. Boudalia, S. Echihi, A. Harmaoui, J. Sebhaoui, H. Elmsellem, A. B. Ben Ali, A. B., Y. Ramli, A. Guenbour, A. Bellaouchou, and E. M. Essassi,. Performance and theoretical study on corrosion inhibition of new Triazolo-pyrimidine derivative for Carbon steel in hydrochloric acid. *Journal of Materials and Environmental Sciencez*, 8(2) (2017) 378-388.

[27] H. F. Chahul, A. M. Ayuba, and S. Nyior, Adsorptive, Kinetic,Thermodynamic and Inhibitive Properties of *Cissus Populnea Stem Extract* on the Corrosion of Aluminum in Acid Medium. *ChemSearch Journal,* 6(1) (2015) 20–30. *Publication of Chemical Society of Nigeria*, Kano Chapter

[28] F. E. Awe, S.O. Idris, M. Abbdulwahab, and E. E.Oguzie, Theoretical and Experimental Inhibitive Properties of Mild Steel in HCl by Ethanolic Extract of *Boscia senegalensis*. *Journal of Material Science.* 41(5) (2015) 337-343.
[29] N. O. Eddy,. Ethanol extract of phyllanthus amarus as green inhibitor for the corrosion of mild steel in H_2SO_4. *portugaliar electrochemical acta* 27(5) (2009) 579-589
[30] E. E. Ebenson, N. O. ddy and A. O Odiongenyi. Corrosion Inhbitive Properties and Adsorption Behavior of Ethanol Extract of *Piper guinensis* as a Green Corrosion Inhibitor for Mild Steel in Sulphuric Acid. *African Journal of Pure and Applied Chemistry.* 2(11) (Year) 107-115.
[31]N.O. Eddy, and E. E. Ebenso. Adsorption and Inhibitive Properties of Ethanol Extracts of *Musa sapientum* peels as a Green Corrosion Inhibitor for Mild Steel in Sulphuric Acid. *African Journal of Pure and Applied Chemistry.* 2(6) (2008) 046-054
[32] H. Zarrok, H. Oudda, A. Zarrouk, R. Salghi, B.Hammouti, and M. Bouachrine, Weight Loss Measurement and Theoretical Study of New Pyridazine Compound asCorrosion Inhibitor for C38 Steel in Hydrochloric Acid Solution. *Der Pharma Chemica,* 3(6) (2011) 576-590.
[33] Z. Zhang, N. C. Tian, X. D. Huang, W. Shang, and L. Wu, (2016). Synergistic inhibitionof carbon steel corrosion in 0.5 M HCl solution by indigo carmine and some cationic organic compounds: Experimental and theoretical studies. *RSC. Advances,* 6(27) (2016) 22250–22268.
[34] K.O. Abiola, N.C. Oforka, E. E. Ebenso, and N.M. Nwinuka, Eco-friendly Corrosion Inhibitors: The Inhibitive Action of *Delonix Regia* Extract for the Corrosion Inhibition of Aluminium in Acidic Media. *Anti-Corrosion Methods and Materials.* 54(4) (2007) *219-224*
[35] N.O. Eddy, and A.O. Odiongenyi, Corrosion Inhibition and Adsorption Properties of Ethanol Extract of *Heinsia crinata* on Mild Steel in Sulphuric Acid. *Emrald Journal of Pigment and Resin Technology.* 39(05) (2010) 285-295.
[36] M. Dahmani, A. Et-Touhami, S.S. Al-Deyab, B. Hammouti, A. Bouyanzer, Corrosion Inhibition of C38 Steel in 1 M HCl: A Comparative Study of Black Pepper Extract and Its Isolated Piperine, *Int. J. Electrochem. Sci.,* 5 (2010) 1060- 1069.
[37] K.M. Emran, N.M. Ahmed, B.A. Torjoman, A.A. Al-Ahmadi, S.N. Sheekh, Cantaloupe Extracts as Eco Friendly Corrosion Inhibitors for Aluminum in acidic and alkaline solutions, *J. Mater. Environ. Sci.* 5 (6) (2014) 1940-1950
[38] A.I. Ali, H.E. Megahed, M.A. El-Etre, M.N. Ismail, Zinc corrosion in HCl in the presence of aqueous extract of Achillea fragrantissima, *J. Mater. Environ. Sci.* 5 (2014) 923-930
[39] D. Bouknana, B. Hammouti, M. Messali, A. Aouniti, M. Sbaa, Phenolic and non-Phenolic Fractions of the Olive Oil Mill Wastewaters as Corrosion Inhibitor for Steel in HCl medium, *Port. Electrochim. Acta,* 32 (2014) 1-19.
[40] N.O. Eddy, and E.E. Ebenso, Adsorption and Inhibitive Properties of Ethanol Extracts of *Musa sapientum* peels as a Green Corrosion Inhibitor for Mild Steel in Sulphuric Acid. *African Journal of Pure and Applied Chemistry.* 2(6) (2008) 046-054
[41] S. Leelavathi, and R. Rajalakshmi, .*Dodonaea viscosa*(L.) Leaves extract as acid Corrosion inhibitor for mild Steel. *Journal of Material and Environmental Science*. 4(5) (2013) 625-638.
[42] Y. Abboud, A. Abourriche T. Saffaj, M. Berrada, M. Charrouf, A. Bennamara, N. Al Himidi, H. Hannache, A novel azo dye, 8-quinolinol-5-azoantipyrine as corrosion inhibitor for mild steel in acidic media *Journal ofMaterial Chemistry Physics.* 118(3) (2007) 295-303.
[43] H. Lgaz, R. Salghi, and I. H. Ali, Corrosion Inhibition Behavior of 9-Hydroxyrisperidone as a Green Corrosion Inhibitor for Mild Steel in Hydrochloric Acid: Electrochemical DFT and MD Simulations Studies.*International Journal of Electrochemical Science.,*13 (2018) 250–264.

[44] M.H. Mahross, K. Efil, T.A .S El-Nasr, and O.A Abbas, Experimental and Theoretical Study on Corrosion Inhibition of Mild Steel in Oilfield Formation Water Using Some Schiff Base Metal Complexes. *Journal of Electrochemical Science and Technology,* 8 (3) (2017) 222-235.

[45] I. Ahamad, R. Prasad, and M.A. Quraishi, Adsorption and Inhibitive Properties of some Mannich Bases of Isatin Derivatives on Corrosion of Mild Steel in Acidic Media. *Corrosion Science*, 52 (2010) 3033-3441.

[46] A.D. Becke, "Density functional thermochemistry. III". The role of exact exchange, *Journal of Chemistry and Physics*. 98 (1993) 5648–6562

[47] H. Cang, F. Zhenghao, S. Wenyan, and X. Qi, Experimental and Theoretical Study forCorrosion Inhibition of Mild Steel by L-Cysteine. *International Journal Of Electrochemical Science.* 7 (2012) 10121 – 10131.

[48] B. Usman. M. Hasmerya, H.H Abdallah, M., Aziz, M. Computational Evaluation of the Effect of Structural Parameters of 3-Fluoro Thiophene and 3-Thiophene Malonic Acid on Corrosion Inhibition efficency of mild steel in acidic media, *International Journal of Electrochemical Science,* 10 (2015) 3223-3229

[49] V.S. Sastri, and J.R. Perumareddi, Molecular orbital theoretical studies of some organic corrosion inhibitors. *JournalCorrosion Science,* 53(8) (1997) 617– 622.

[50] L. Guo, R. Xiaolei, Z. Yang, X. Shenying, and g. Yulong, G. and Shengtao, Z. Theoretical evaluation of the corrosion inhibition performance of 1,3-thiazole and its amino derivatives. *Arabian Journal of Chemistry.* 10 (2017) 121–130

[51] A. N.Wazzan, R. H. Albrakaty, and I. B. Obot, Theoretical Study of the Mechanism of Corrosion Inhibition of Carbon Steel in Acidic Solution by 2-aminobenzothaizole and 2-Mercatobenzothiazole. *International Journal Electrochemical Science.*13 (2018) 3535 – 3554

[52] R. G. Parr, L. Von-Szentpaly, S.B. Liu, Electrophilicity index, *Journal of American Chemical Society.* 121(9) (1999)1922–1924.

[53] G. Bereket, C. Öğretir, and & Özşahin, Ç. Quantum chemical studies on the inhibition efficiencies of some piperazine derivatives for the corrosion of steel in acidic medium. *Journal molecular Structure*.: 663: (2003) 39–46.

[54] M Behpour, Electrochemical and theoretical investigation on the corrosion inhibition of mild steel by thiosalicylaldehyde derivatives in hydrochloric acid solution. *journal of Corrosion. Scienc*e. 50 (2008) 2172–2181,

[55] T. Arslan, F. Kandemirli, E. E. Ebenso, I. Love, and H Alemu.. Quantum chemical studies on the corrosion inhibition of some sulphonamides on mild steel in acidic medium. *Journal of Corrosion Science* 51 (2009) 35–47

[56] L.C. Murulana, A.K. Singh, S.K. Shukla, M.M. Kabanda, and E.E. Ebenso, Experimental and quantum chemical studies of some bis (trifluoromethyl-sulfonyl) imide imidazolium-based ionic liquids as corrosion inhibitors for mild steel in hydrochloric acid solution. *Industrial and Engineering Chemical Research*. 51 (2012) 13282–13299.

[57] M.M. Kabanda, I.B. Obot, and E. E. Ebenso, Computational study of some amino acid derivatives as potential corrosion inhibitors for different metal surfaces and in different media. *Internatinal Journal of Electrochemical. Science*. 8 (2013) 10839–10850

[58] M. E Mashuga, Adsorption, thermodynamic and quantum chemical studies of 1-hexyl-3-methylimidazolium based ionic liquids as corrosion inhibitors for mild steel in HCl. *Journal of Material Science* 8, (2015) 3607–3632

[59] K. Kathirvel, T. Brindha, and J. Mallika, Quantum Chemical Studies on the Corrosion Inhibition of Mild Steel by Piperidin-4-One Derivatives in 1M H_3PO_4. *Open Journal of Metal*. 4 (2014) 73-85.

[60] Z. Zhang, N.C. Tian, X.D Huang, W. Shang, and L. Wu, Synergistic inhibitionof carbon steel corrosion in 0.5 M HCl solution by indigo carmine and some cationic organic compounds: Experimental and theoretical studies. *RSC. Advances,* 6(27) (2016) 22250–22268.

[61] T. E. Odetoye, J. Titiloye, and J. O. Ighalo, "A Thermodynamic Study Of Rice Husk (Oryza Sativa) Pyrolysis," *European Journal of Sustainable Development Research,* 3 (2019) 1-10.

[62] B. Usman, H. Maarf, H. H. Abdallah and M. Aziz, Evaluation of 2-Thiophene carbonitrile as corrosion inhibitor on mild steel. *Journal of matrials and Enviromental Science* 9(9) (2018) 2678-2685

[63] A. Usman, H. U. Farouk and U. Bishir. Inhibiton perfomance of cameldung extract on the corrosion of mild in hydrochloric acid. *Algerian Journal of Material Chemistry,* 3(2) (2020) 77-89